Science
AAAS

Dynamic Ca2+-Dependent Stimulation of Vesicle Fusion by Membrane-Anchored Synaptotagmin 1
Han-Ki Lee, *et al.*
Science **328**, 760 (2010);
DOI: 10.1126/science.1187722

Science (print ISSN 0036-8075; online ISSN 1095-9203) is published weekly, except the last week in December, by the American Association for the Advancement of Science, 1200 New York Avenue NW, Washington, DC 20005.

checkpoints to ensure fidelity have been demonstrated in transfer RNA synthetases (*27*), protein synthesis (*28*), and DNA and RNA polymerases (*29*, *30*) and possibly represent a general principle for complex cellular pathways that need to recognize degenerate signals or to discriminate between correct and incorrect substrates based on minor differences.

References and Notes

1. P. Walter, A. E. Johnson, *Annu. Rev. Cell Biol.* **10**, 87 (1994).
2. T. A. Rapoport, *Nature* **450**, 663 (2007).
3. M. Halic *et al.*, *Nature* **444**, 507 (2006).
4. M. Halic *et al.*, *Science* **312**, 745 (2006).
5. C. Schaffitzel *et al.*, *Nature* **444**, 503 (2006).
6. M. R. Pool, J. Stumm, T. A. Fulga, I. Sinning, B. Dobberstein, *Science* **297**, 1345 (2002).
7. X. Zhang, S. Kung, S. O. Shan, *J. Mol. Biol.* **381**, 581 (2008).
8. X. Zhang, C. Schaffitzel, N. Ban, S. O. Shan, *Proc. Natl. Acad. Sci. U.S.A.* **106**, 1754 (2009).
9. T. Connolly, R. Gilmore, *Cell* **57**, 599 (1989).
10. D. Huber *et al.*, *J. Bacteriol.* **187**, 2983 (2005).
11. J. W. De Gier, Q. A. Valent, G. Von Heijne, J. Luirink, *FEBS Lett.* **408**, 1 (1997).
12. Q. A. Valent *et al.*, *EMBO J.* **14**, 5494 (1995).
13. S. K. Doud, M. M. Chou, D. A. Kendall, *Biochemistry* **32**, 1251 (1993).
14. Materials and methods are available as supporting material on *Science* Online.
15. Single-letter abbreviations for the amino acid residues are as follows: A, Ala; C, Cys; D, Asp; E, Glu; F, Phe; G, Gly; H, His; I, Ile; K, Lys; L, Leu; M, Met; N, Asn; P, Pro; Q, Gln; R, Arg; S, Ser; T, Thr; V, Val; W, Trp; and Y, Tyr.
16. J. H. Peterson, R. L. Szabady, H. D. Bernstein, *J. Biol. Chem.* **281**, 9038 (2006).
17. C. Schaffitzel, N. Ban, *J. Struct. Biol.* **158**, 463 (2007).
18. T. Bornemann, J. Jöckel, M. V. Rodnina, W. Wintermeyer, *Nat. Struct. Mol. Biol.* **15**, 494 (2008).
19. C. G. Jensen, S. Pedersen, *J. Bacteriol.* **176**, 7148 (1994).
20. J. J. Flanagan *et al.*, *J. Biol. Chem.* **278**, 18628 (2003).
21. I. Buskiewicz *et al.*, *Proc. Natl. Acad. Sci. U.S.A.* **101**, 7902 (2004).
22. N. Zheng, L. M. Gierasch, *Cell* **86**, 849 (1996).
23. J. D. Miller, H. D. Bernstein, P. Walter, *Nature* **367**, 657 (1994).
24. T. Powers, P. Walter, *EMBO J.* **16**, 4880 (1997).
25. S. O. Shan, S. Chandrasekar, P. Walter, *J. Cell Biol.* **178**, 611 (2007).
26. R. S. Hegde, S. W. Kang, *J. Cell Biol.* **182**, 225 (2008).
27. A. R. Fersht, M. M. Kaethner, *Biochemistry* **15**, 3342 (1976).
28. M. V. Rodnina, W. Wintermeyer, *Annu. Rev. Biochem.* **70**, 415 (2001).
29. T. A. Kunkel, K. Bebenek, *Annu. Rev. Biochem.* **69**, 497 (2000).
30. S. M. Uptain, C. M. Kane, M. J. Chamberlin, *Annu. Rev. Biochem.* **66**, 117 (1997).

31. We thank C. Schaffitzel and N. Ban for help with the purification of RNCs and Trigger factor; J. Luirink for plasmids encoding the phoA signal sequence variants; L. Randall for the plasmid encoding luciferase; B. Bukau and E. Deuerling for the plasmid encoding Trigger factor; F. Nataro for the plasmid encoding EspP; H. D. Bernstein for the strain HDB51; and R. J. Deshaies, A. Varshavsky, W. Zhong, N. Pierce, and the Shan laboratory for comments on the manuscript. This work was supported by NIH grant GM078024, and career awards from the Burroughs Wellcome Foundation, the Henry and Camille Dreyfus Foundation, the Arnold and Mabel Beckman Foundation, and the Packard Foundation to S.S.

Supporting Online Material

www.sciencemag.org/cgi/content/full/328/5979/757/DC1
Materials and Methods
SOM Text
Table S1
Figs. S1 to S9
References

6 January 2010; accepted 18 March 2010
10.1126/science.1186743

Dynamic Ca^{2+}-Dependent Stimulation of Vesicle Fusion by Membrane-Anchored Synaptotagmin 1

Han-Ki Lee,[1]* Yoosoo Yang,[3]* Zengliu Su,[4]* Changbong Hyeon,[5] Tae-Sun Lee,[1] Hong-Won Lee,[1] Dae-Hyuk Kweon,[3] Yeon-Kyun Shin,[4,6]† Tae-Young Yoon[1,2]†

In neurons, synaptotagmin 1 (Syt1) is thought to mediate the fusion of synaptic vesicles with the plasma membrane when presynaptic Ca^{2+} levels rise. However, in vitro reconstitution experiments have failed to recapitulate key characteristics of Ca^{2+}-triggered membrane fusion. Using an in vitro single-vesicle fusion assay, we found that membrane-anchored Syt1 enhanced Ca^{2+} sensitivity and fusion speed. This stimulatory activity of membrane-anchored Syt1 dropped as the Ca^{2+} level rose beyond physiological levels. Thus, Syt1 requires the membrane anchor to stimulate vesicle fusion at physiological Ca^{2+} levels and may function as a dynamic presynaptic Ca^{2+} sensor to control the probability of neurotransmitter release.

Intracellular membrane trafficking in eukaryotic cells involves fusion of membrane-bounded compartments (*1*) and is mediated by the SNARE (soluble N-ethylmaleimide–sensitive factor attachment protein receptor) proteins found on both the vesicle (v-SNARE) and target membranes (t-SNARE) (*2*–*4*). In neurons, synaptotagmin 1 (Syt1) is a Ca^{2+} sensor that interacts with SNAREs and membranes to mediate synaptic vesicle fusion, triggering synchronous neurotransmission (*3*, *5*, *6*). Proteoliposome fusion mediated by the t- and v-SNARE proteins is a useful in vitro system (*7*) for dissecting the molecular functions of presynaptic fusion regulators, including Syt1 (*5*, *6*, *8*). The soluble Syt1 variant, which has the two cytoplasmic C2 domains but lacks the transmembrane domain, has been the subject of extensive studies (*9*–*14*). This "soluble C2AB" accelerates proteoliposome fusion to reach a time constant of about 10 s when 100 μM or 1 mM Ca^{2+} is added (*13*, *14*). However, when the full-length, membrane-anchored Syt1 is used, addition of the same levels

[1]Department of Physics, KAIST, Daejeon 305-701, South Korea. [2]Institute for the BioCentury, KAIST, Daejeon 305-701, South Korea. [3]Department of Genetic Engineering, Sungkyunkwan University, Suwon, Gyeonggi-do 440-746, South Korea. [4]Department of Biochemistry, Biophysics, and Molecular Biology, Iowa State University, 4152 Molecular Biology Building, Ames, IA 50011, USA. [5]School of Computational Sciences, Korea Institute for Advanced Study, Seoul 130-722, South Korea. [6]Division of Integrative Biosciences and Biotechnology, POSTECH, Pohang 790-784, South Korea.

*These authors contributed equally to this work.
†To whom correspondence should be addressed. E-mail: colishin@iastate.edu (Y.-K.S.); tyyoon@kaist.ac.kr (T.-Y.Y.)

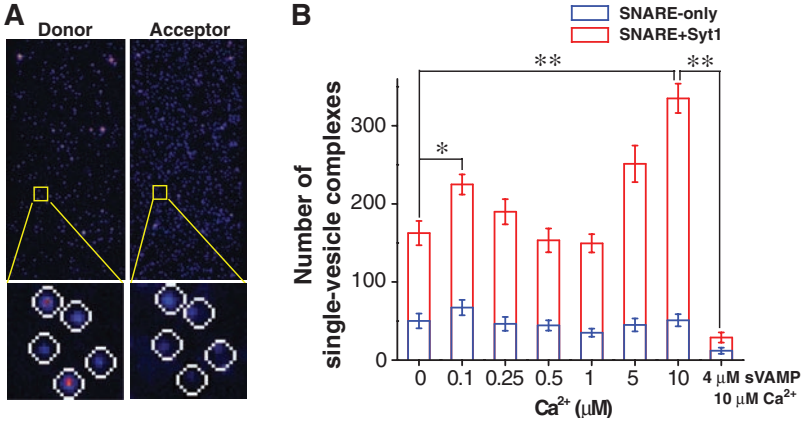

Fig. 1. Membrane-anchored Syt1 stimulates single-vesicle docking using 10 μM Ca^{2+}. (**A**) Exemplary images of single-vesicle FRET imaging. Fluorescence signals from single-vesicle complexes were separated with the threshold at 645 nm and detected as the donor and the acceptor channel signals, respectively (top). Each single-vesicle complex appearing as a Gaussian peak is identified (bottom). (**B**) Number of single-vesicle complexes formed between t- and v-vesicles under the conditions depicted. The surface-immobilized v-vesicles contain both v-SNARE and Syt1 (red bar) or only v-SNAREs (blue bar). *$P < 0.05$ and **$P < 0.01$, assessed using the paired t test, and all the errors are SD unless otherwise specified.

of Ca^{2+} instead inhibits fusion (*12*, *15*, *16*). This membrane anchor is preserved in all isoforms of the Syt family except Syt17 (*17*), suggesting that it plays an important role in regulating synaptic vesicle fusion. Understanding this currently hidden role of the membrane anchor requires the study of Ca^{2+}-evoked vesicle fusion stimulated by membrane-anchored Syt1.

Here, we used a single-vesicle fluorescence fusion assay to track the time course of individual vesicle-vesicle fusion events (fig. S1) (*18*, *19*). The assay involves one group of vesicles (called

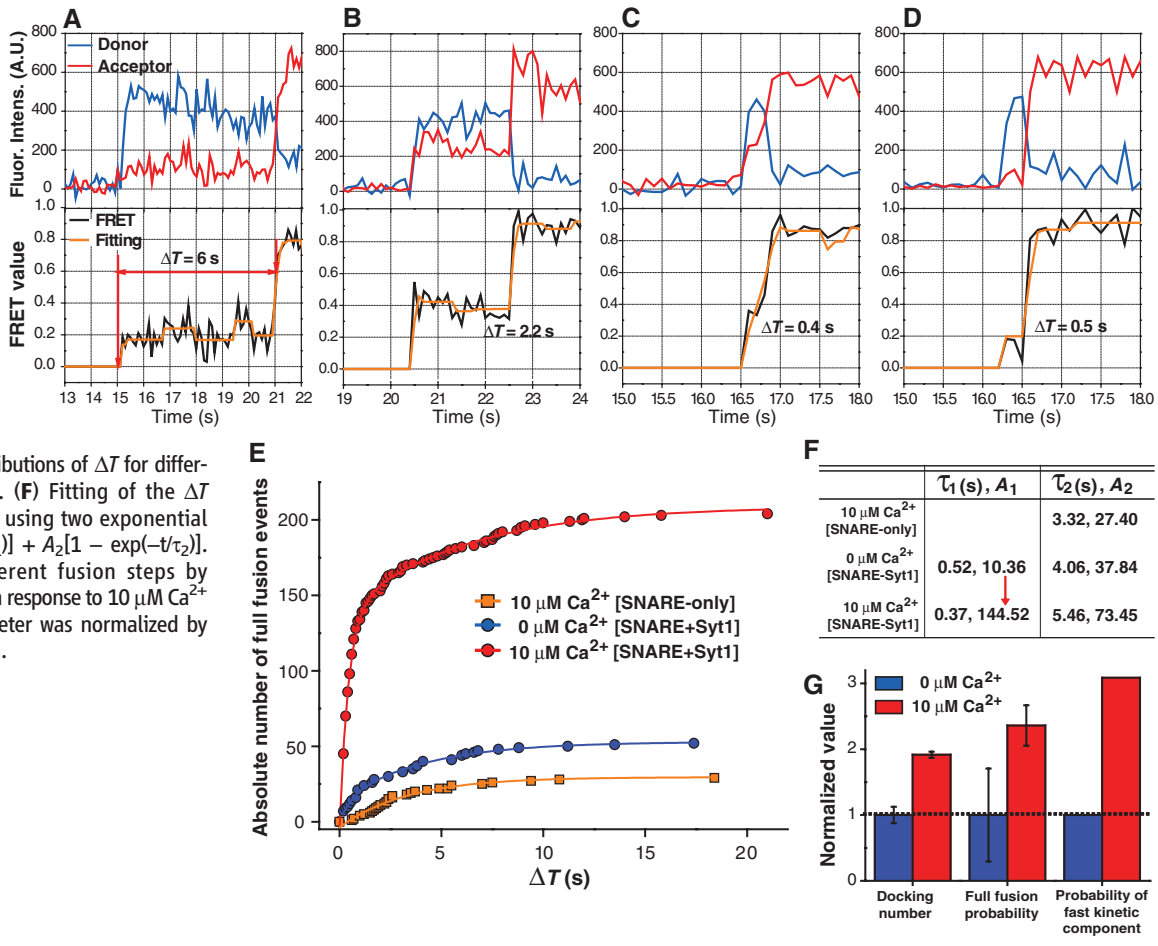

Fig. 2. Membrane-anchored Syt1 catalyzes full fusion on the hundreds of ms scale in response to 10 μM Ca^{2+}. (**A** to **D**) Exemplary real-time traces of single-vesicle fusion events. (Top) The changes in the donor (blue) and acceptor (red) fluorescence intensities. (Bottom) The corresponding changes in FRET (black) and stepwise increases in the FRET signals identified by Schwarz information criterion (orange). (**E**) Cumulative distributions of ΔT for different molecular conditions. (**F**) Fitting of the ΔT distributions shown in (E) using two exponential functions: $A_1[1 - \exp(-t/\tau_1)] + A_2[1 - \exp(-t/\tau_2)]$. (**G**) Acceleration of different fusion steps by membrane-anchored Syt1 in response to 10 μM Ca^{2+} (SOM text 1). Each parameter was normalized by that of 0 μM Ca^{2+} reaction.

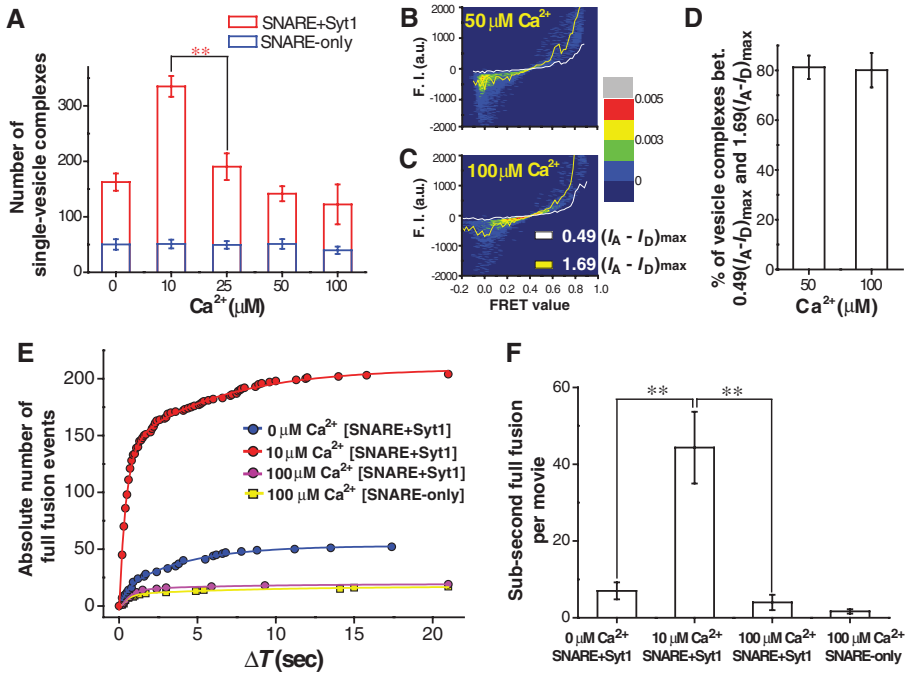

Fig. 3. Membrane-anchored Syt1 is inactivated at sub-mM Ca^{2+} levels. (**A**) Docking-number analysis for the Ca^{2+} range between 10 and 100 μM Ca^{2+}. (**B** to **D**) Fluorescence intensity analysis of the single-vesicle complexes. Single-vesicle complexes are placed on the graph plane (FRET efficiency, $I_A - I_D$) to make a density plot (SOM text 2). The percentages of single-vesicle complexes between white and yellow lines, $0.49(I_A - I_D)_{max}$ and $1.69(I_A - I_D)_{max}$ (rough estimates for 30% difference in size), are 81.2% (50 μM) and 80.5% (100 μM Ca^{2+}) (D). (**E**) Cumulative distributions of ΔT of single-vesicle fusion events for different molecular conditions (each based on three independent real-time movies). The total docking numbers are 1166 (blue), 2232 (red), 1010 (purple), and 1272 (yellow), respectively. (**F**) The absolute number of subsecond full-fusion events ($\Delta T < 1$ s) per imaging area, for different protein compositions and Ca^{2+} concentrations.

v-vesicles), containing v-SNARE, full-length Syt1 and lipidic acceptor dyes, immobilized on an imaging surface. A second group of vesicles (t-vesicles), with the precomplex of t-SNAREs and lipidic donor dyes, are mixed with a desired concentration of Ca^{2+} and introduced for reaction via microfluidic buffer exchange. When the t-vesicles react with the surface-immobilized v-vesicles, a single-vesicle complex is formed that can be detected by an increase in the efficiency of the fluorescence resonance energy transfer (FRET) between the donor and acceptor dyes. Docking between t- and v-vesicles generates a FRET efficiency of less than 0.2, whereas the fully fused state generates 0.75 or higher (*18*).

We first analyzed the ability of membrane-anchored Syt1 to stimulate SNARE-mediated single-vesicle docking using μM Ca^{2+} levels. After a 3-s reaction between the t- and v-vesicles, we counted the number of single-vesicle complexes formed per imaging area (Fig. 1A and figs. S2 to S5). In the absence of Ca^{2+}, Syt1 increased the docking number by a factor of three (Fig. 1B). The stimulation of docking by Syt1 was Ca^{2+}-dependent, and there was another two-fold enhancement between 0 and 10 μM Ca^{2+} (Fig. 1B). We also tested whether this Syt1 effect on docking was strictly dependent on SNARE activity. We disabled the t-SNAREs using a SNARE-motif peptide of v-SNARE (sVAMP), which suppressed the docking number by as much as 90% (Fig. 1B). This observation indicates that Syt1's stimulation essentially involves formation of the ternary SNARE complexes (*20*–*22*).

To control the late steps of neurotransmitter release, Syt1 should have the capacity to catalyze the transition to the full-fusion state (*3*, *5*, *6*). To explore this possibility, we employed a real-time tracking approach, which followed the entire course of fusion events occurring in individual single-vesicle complexes (Fig. 2, A to D, fig. S6, and movie S1). The time gap between the docking and full fusion, Δ*T*, exclusively measured the full-fusion kinetics of an individual fusion event, separated from the docking kinetics (Fig. 2, A to D, and SOM text 1). When the v-vesicle contained only v-SNAREs, the cumulative plot of Δ*T* shows a single exponential distribution [three independent movies used for each plot (Fig. 2, E and F)]. Inclusion of Syt1 without Ca^{2+} (Fig. 2E) created a small, fast-kinetic component (Fig. 2F, τ_1 = 520 ms). When we added 10 μM Ca^{2+} to this reaction with membrane-anchored Syt1 (Fig. 2E), the absolute population of the fast-kinetic component increased by a factor of 14 (Fig. 2F). This increase of the fast component was not simply due to docking enhancement, but rather was the result of direct acceleration of the full-fusion kinetics (Fig. 2G and SOM text 1). Although it was shown that lipid mixing could occur without proper mixing of contents (*23*), this fast-fusion kinetics provides convincing evidence that we have observed actual fusion events rather than slow lipid rearrangements such as flip-flop transitions. Thus, in response to 10 μM Ca^{2+}, the membrane-anchored Syt1 directly accelerates the full-fusion reaction, in addition to the docking kinetics.

To determine what happens when the Ca^{2+} concentration increases beyond 10 μM, we repeated the docking-number analysis while increasing Ca^{2+} to 100 μM (Fig. 3, A to D). Unexpectedly, the population of single-vesicle complexes that peaked at 10 μM Ca^{2+} dropped as the Ca^{2+} level rose further, which was visible at 25 μM Ca^{2+} (Fig. 3A). At 100 μM Ca^{2+}, the docking number became comparable to that obtained with no Ca^{2+} (Fig. 3A). In addition, the fluorescence intensity analyses excluded the possibility of multiple-vesicle aggregation at high Ca^{2+} concentrations (Fig. 3, B to D, and SOM text 2). We also performed real-time tracking measurements with higher Ca^{2+} and found that 100 μM Ca^{2+} indeed cut down the catalysis of full-fusion states (Fig. 3E); the absolute population showing a full-fusion event was smaller than that of the 0 μM Ca^{2+} reaction and similar to that observed for the SNARE-only reaction without Syt1 (Fig. 3E). Thus, at 100 μM Ca^{2+}, membrane-anchored Syt1 is largely deactivated and loses its capacity to catalyze the full-fusion state (Fig. 3F).

To study the physical mechanism of Syt1 activity (Fig. 4), we weakened the interaction between Syt1 and the cis-membrane by removing negatively charged phosphatidylserine (PS) lipids from the v-vesicle membrane (*9*, *12*, *24*). Without the PS lipids in the cis-membrane, the docking stimulation by Syt1 lost the tendency to decrease up to 100 μM Ca^{2+} (Fig. 4A). On the other hand, when we decreased the phosphatidylinositol 4,5-bisphosphate (PIP_2) lipids in the t-vesicle membrane from 6 (*25*) to 0.5 mole percent (mol %), the stimulatory effect of Syt1 was abolished in the entire Ca^{2+} range studied (Fig. 4A).

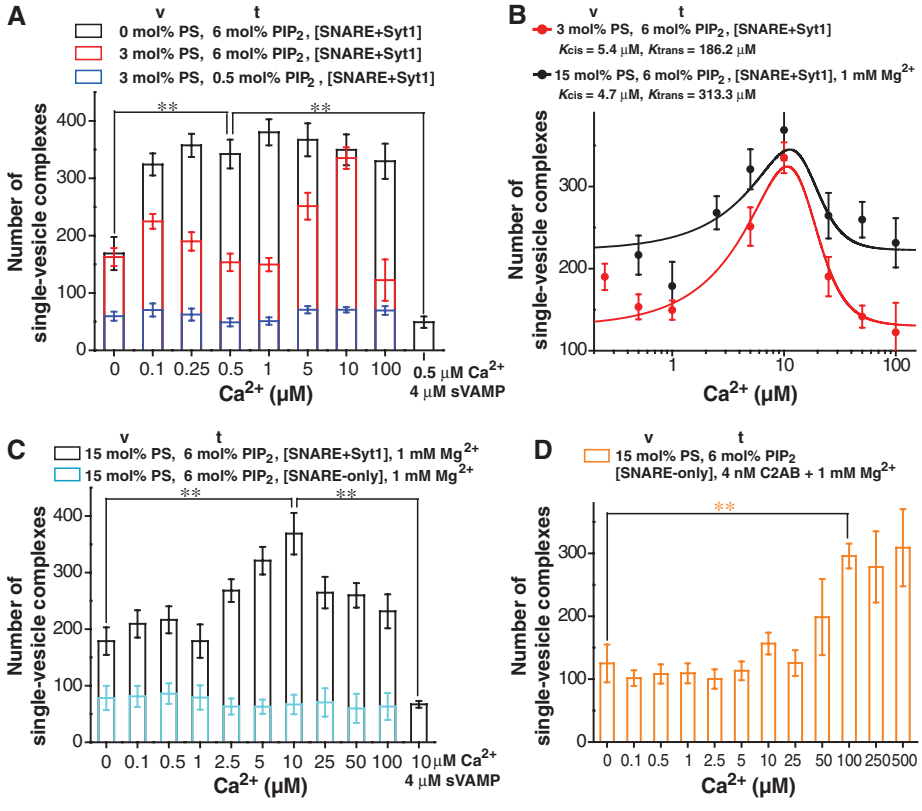

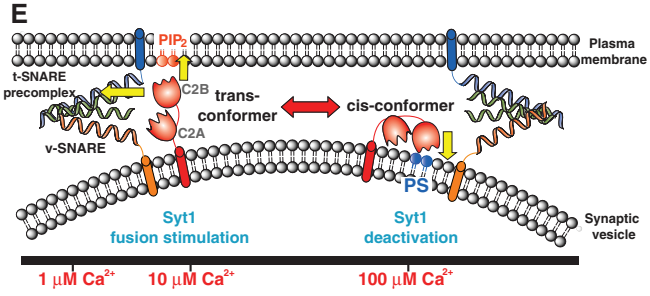

Fig. 4. Dynamic Ca^{2+}-dependent stimulation of vesicle fusion by membrane-anchored Syt1. (**A** to **D**) Single-vesicle docking data under the molecular conditions depicted for the cis (v-vesicle) and trans (t-vesicle) membranes. Reactions are carried out with the membrane-anchored Syt1 in the cis-membrane [(A to (C)] or soluble C2AB in the fusion buffer (D) (see SOM text 4). Theoretical fitting of the docking-number data using a modified MWC model (B) (SOM text 3). 15 mol % PS lipids are included for the trans-membrane in every case. (**E**) Molecular model for the activity of the membrane-anchored Syt1.

Thus, Syt1 needs to interact with both the t-SNARE precomplex (Figs. 1B and 4A, sVAMP treatment) and PIP_2 on the transmembrane for its stimulatory effect, whereas the folding back of Syt1 to the cis-membrane causes its inactivation (Fig. 4E) (*12*, *24*).

The data also suggest that the balance of Syt1's cis- and trans-membrane interactions shifts dynamically as a function of Ca^{2+} concentration. From the single-vesicle data (Fig. 4A), we presume two conformations of Syt1, cis- and trans-conformers, where only the trans-conformer stimulates fusion (SOM text 3 and fig. S7). The Ca^{2+}-dependent power shift between these two conformers could be explained by assigning different Ca^{2+} dissociation constants to the cis- (K_{cis}) and trans-conformers (K_{trans}) (Fig. 4B), reminiscent of the classical Monod-Wyman-Changeux (MWC) model for protein allostery. Our model predicts a large anisotropy in the two dissociation constants; $K_{trans}/K_{cis} \approx 34$ (Fig. 4B), indicating that at high Ca^{2+} levels where $[Ca^{2+}]/K_{cis} >> 1$, Syt1 predominantly partitions into the cis-conformer and becomes inactivated (Fig. 4E). Because the C2B domain exhibits a much larger Ca^{2+}-binding dissociation constant (*5*, *10*, *26*), it is tempting to speculate that the trans-conformer, critical for fusion stimulation, is predominantly mediated by the C2B domain.

Finally, we observed that the presence of another divalent ion, Mg^{2+}, affected the overall shape of the Ca^{2+}-dependent stimulation pattern. Simply increasing the PS lipids in the cis-membrane to the physiological level of 15 mol % (*27*) pushed the stimulation peak to sub-μM Ca^{2+} levels, followed by a quick deactivation of Syt1 that began at 1 μM Ca^{2+} (fig. S8A). However, in the presence of physiological 1 mM Mg^{2+}, the stimulation peak at 10 μM Ca^{2+} was restored (Fig. 4, B and C), probably due to the enhanced screening of electrostatic interactions by Mg^{2+} ions. Furthermore, this nonmonotonic docking pattern correlated well with up- and down-regulation of the ability of Syt1 to accelerate the full-fusion kinetics (fig. S8, B and C). Thus, the essential molecular activities of membrane-anchored Syt1 can be reproduced under physiological charge conditions in the cis- and trans-membranes. Synaptic vesicles directly isolated from rat brain, which have native Syt1 and lipids, also show a deactivation behavior at 100 μM and 1 mM Ca^{2+} (*16*). These observations collectively suggest that the dynamic Ca^{2+}-dependent activity of Syt1 would occur in physiological contexts.

We have demonstrated that anchoring Syt1 to a lipid membrane fundamentally changes its molecular activity. In the presynaptic active zone, tens of μM or even several μM of presynaptic Ca^{2+} is sufficient to trigger strong neurotransmitter release (*28*, *29*). The membrane-anchored Syt1 reconstituted in our assay has a remarkable Ca^{2+} sensitivity, responding to those Ca^{2+} levels operational at the presynaptic termini. In comparison, at the same effective concentration, we found that the soluble C2AB required one order of magnitude higher Ca^{2+} for docking stimulation and did not show any deactivation pattern up to 500 μM Ca^{2+} (SOM text 4). Thus, in addition to the enhanced Ca^{2+} sensitivity, Syt1's membrane anchor seems to give it the Ca^{2+}-dependent, nonmonotonic activity. A simple use of sub-mM Ca^{2+} only inactivates membrane-anchored Syt1, which may explain why previous in vitro studies failed to observe stimulatory effects with full-length Syt1. Our work suggests that Syt1 modulates the probability of neurotransmitter release in response to the presynaptic Ca^{2+} levels and molecular composition of membranes, which may contribute to the dynamic plasticity of neuronal communication.

Reference and Notes

1. J. S. Bonifacino, B. S. Glick, *Cell* **116**, 153 (2004).
2. J. E. Rothman, *Nature* **372**, 55 (1994).
3. T. C. Sudhof, *Annu. Rev. Neurosci.* **27**, 509 (2004).
4. R. Jahn, R. H. Scheller, *Nat. Rev. Mol. Cell Biol.* **7**, 631 (2006).
5. E. R. Chapman, *Annu. Rev. Biochem.* **77**, 615 (2008).
6. J. Rizo, C. Rosenmund, *Nat. Struct. Mol. Biol.* **15**, 665 (2008).
7. T. Weber *et al.*, *Cell* **92**, 759 (1998).
8. A. T. Brunger, K. Weninger, M. Bowen, S. Chu, *Annu. Rev. Biochem.* **78**, 903 (2009).
9. W. C. Tucker, T. Weber, E. R. Chapman, *Science* **304**, 435 (2004).
10. D. Araç *et al.*, *Nat. Struct. Mol. Biol.* **13**, 209 (2006).
11. S. Martens, M. M. Kozlov, H. T. McMahon, *Science* **316**, 1205 (2007).
12. A. Stein, A. Radhakrishnan, D. Riedel, D. Fasshauer, R. Jahn, *Nat. Struct. Mol. Biol.* **14**, 904 (2007).
13. M. Xue, C. Ma, T. K. Craig, C. Rosenmund, J. Rizo, *Nat. Struct. Mol. Biol.* **15**, 1160 (2008).
14. E. Hui, C. P. Johnson, J. Yao, F. M. Dunning, E. R. Chapman, *Cell* **138**, 709 (2009).
15. L. K. Mahal, S. M. Sequeira, J. M. Gureasko, T. H. Söllner, *J. Cell Biol.* **158**, 273 (2002).
16. M. Holt, D. Riedel, A. Stein, C. Schuette, R. Jahn, *Curr. Biol.* **18**, 715 (2008).
17. M. Craxton, *BMC Genomics* **8**, 259 (2007).
18. T. Y. Yoon, B. Okumus, F. Zhang, Y. K. Shin, T. Ha, *Proc. Natl. Acad. Sci. U.S.A.* **103**, 19731 (2006).
19. T. Y. Yoon *et al.*, *Nat. Struct. Mol. Biol.* **15**, 707 (2008).
20. X. Zhang, M. J. Kim-Miller, M. Fukuda, J. A. Kowalchyk, T. F. Martin, *Neuron* **34**, 599 (2002).
21. A. Bhalla, M. C. Chicka, W. C. Tucker, E. R. Chapman, *Nat. Struct. Mol. Biol.* **13**, 323 (2006).
22. H. de Wit *et al.*, *Cell* **138**, 935 (2009).
23. Y. H. Chan, B. van Lengerich, S. G. Boxer, *Proc. Natl. Acad. Sci. U.S.A.* **106**, 979 (2009).
24. J. Bai, W. C. Tucker, E. R. Chapman, *Nat. Struct. Mol. Biol.* **11**, 36 (2004).
25. D. J. James, C. Khodthong, J. A. Kowalchyk, T. F. Martin, *J. Cell Biol.* **182**, 355 (2008).
26. E. Hui, J. Bai, E. R. Chapman, *Biophys. J.* **91**, 1767 (2006).
27. S. Takamori *et al.*, *Cell* **127**, 831 (2006).
28. R. Schneggenburger, E. Neher, *Curr. Opin. Neurobiol.* **15**, 266 (2005).
29. J. Sun *et al.*, *Nature* **450**, 676 (2007).

T.-Y.Y. thanks W. Bae and J. Ryu for writing analysis programs, K. Kim for help with the supporting movie, and T. Ha and W. Jones for critical reading of the manuscript. This work was supported by Korea Research Foundation grants (KRF-2008-313-C00365 to T.-Y.Y.; KRF-C00142 and KRF-C00180 to C.H.), and National Research Foundation of Korea grants funded by the Korean government (2009-0087691 to T.-Y.Y.; R01-2008-000-10920-0 to C.H.; 2007-D00243 to D.-H.K.). This work was also supported by a National Institutes of Health grant (R01 GM051290 to Y.-K.S.) and the World Class University program in Korea (R31-2008-000-10105-0 to Y.-K.S. and R33-10163 to T.-Y.Y.).

Supporting Online Material

www.sciencemag.org/cgi/content/full/328/5979/760/DC1
Materials and Methods
SOM Text
Figs. S1 to S9
Table S1
Movie S1
References

1 February 2010; accepted 22 March 2010
10.1126/science.1187722